PUBLICATION

MUSTANG

A MUltiple Space and Time scale Approach for the quaNtification of deep saline formations for CO_2 storaGe

Project Number:227286

AUTHORS: Christopher I. McDermott · Alexander E. Bond ·Wenqing Wang · Olaf Kolditz

TITLE: Front Tracking Using a Hybrid Analytical Finite Element Approach for Two-Phase Flow Applied to Supercritical CO2 Replacing Brine in a Heterogeneous Reservoir and Caprock

The research leading to these results has received funding from the European Community's Seventh Framework Programme [FP7/2007/2013) under grant agreement n° [227286]

Status	AUTHOR VERSION
Date	Received: 28 October 2010 / Accepted: 24 June 2011
Publisher	Springer Science+Business Media B.V.
Reference	Transport in Porous Media Journal (Volume 1 / 1986 - Volume 89 / 2011) DOI 10.1007/s11242-011-9799-5 http://dx.doi.org/10.1007/s11242-011-9799-5

Front Tracking using a Hybrid Analytical Finite Element Approach for Two Phase Flow Applied to Supercritical CO_2 Replacing Brine in a Heterogeneous Reservoir and Caprock.

Christopher I McDermott

Edinburgh Collaborative of Subsurface Science and Engineering (ECOSSE), School of Geoscience, University of Edinburgh, West Mains Road, Edinburgh, EH9 3JW, Scotland

Email cmcdermo@staffmail.ed.ac.uk

Alexander E Bond

Quintessa Ltd., Chadwick House, Birchwood Park, Warrington, Cheshire, UK, WA3 6AE

Email alexbond@quintessa.org

Wenqing Wang

Helmholtz Center for Environmental Research, Leipzig, Germany

Technische Universität Dresden, Applied Environmental System Analysis, Germany

Email wenqing.wang@ufz.de

Olaf Kolditz

Helmholtz Center for Environmental Research, Leipzig, Germany

Technische Universität Dresden, Applied Environmental System Analysis, Germany

Email olaf.kolditz@ufz.de

Abstract

Predicting fluid replacement by two phase flow in heterogeneous porous media is of importance for issues such as supercritical CO_2 sequestration, the integrity of caprocks and the operation of oil water/brine systems. When considering coupled process modelling, the location of the interface is of importance as most of the significant interaction between processes will be happening there. Modelling two phase flow using grid based techniques presents a problem as the fluid-fluid interface location is approximated across the scale of the discretisation. Adaptive grid methods allow the discretisation to follow the interface through the model, but are computationally expensive and make coupling to other processes (Thermal, Mechanical, Chemical) complicated due to the constant alteration in grid size and effects thereof. Interface tracking methods have been developed that apply sophisticated reconstruction algorithms based on either the ratio of volumes of a fluid in an element (Volume of Fluid Methods) or the advective velocity of the interface throughout the modelling regime (Level Set Method). In this paper we present an "Analytical Front Tracking" method where a generic analytical solution for two phase flow is used to "add information" to a finite element model. The location of the front within individual geometrical elements is predicted using the saturation values in the elements and the velocity field of the element. This removes the necessity for grid adaptation, and reduces the need for assumptions as to the shape of the interface as this is predicted by the analytical solution. The method is verified against a standard benchmark solution and then applied to the case of CO_2 pooling and forcing its way into a heterogeneous caprock, replacing hot brine and eventually breaking through.

Key words

Two phase flow; Hybrid analytical numerical; CO_2 sequestration; Caprock integrity; Front tracking.

Notation

A	Area of element normal to the fluid flux (m^2)
$A_{2D}^{'}$	2D local coordinate system
A_{3D}^{g}	3D global coordinate system
A_{ne}	Area of influence assigned to a node in the element (m^2)
C_{ij}^{e}	Element storage matrix
C_{ij}	Global storage matrix
D_{t_n}	Distance from an origin at time step n (m)
D_{front}	Distance of a node normal to the saturation front (m)
D_{node}	Distance of a node to the saturation front (m)
$D1_{front}$	Distance of node with S_{max} normal to the saturation front (m)
$D2_{front}$	Distance of node with S_{mid} normal to the saturation front (m)
f_1	Flow rate of phase 1 into or out of a volume (m^3/s)
f_{1i}	Flow rate of phase 1 into or out of a volume discretised to node i (m^3/s)
$f_{\alpha i}^{e}$	Element contribution to flow rate of phase α discretised node i (m^3/s)
g	Acceleration due to gravity (m/s^2)
i, j, k	Iteration integers
$k_{r\alpha}$	Relative permeability of phase α (-)
$\mathbf{k}$	Intrinsic permeability tensor (m^2)
md	Maximum distance predicted by analytical solution from origin (m)
$MN\beta$	Shape function for the node, β =1 for node S_{max} to β =3 for node S_{min}
n_β	Node number β
ne	Number of elements
nn	Number of nodes
P_{Smax}	Global point coordinates for node with maximum saturation in element
p_α	Fluid pressure of phase α (Pa)
p_1, p_2	Fluid pressure of phases 1 and 2 (Pa)
p_c	Capillary pressure (Pa)
p_w	Fluid pressure of phase of wetting phase (Pa)
Q_{total}	Total flow rate of all phases (m^3/s)
Q_1	Flux of phase 1 (m/s)
q_{total}	Total Darcy flow velocity of all phases (m/s)
$\mathbf{q}_\alpha$	Fluid velocity vector (m/s)
$\mathbf{q}'$	Fluid velocity vector in local coordinates (m/s)
S_1	Saturation of fluid phase 1 (-)
S_2	Saturation of fluid phase 2 (-)
S_α	Saturation of fluid phase α ($\alpha = 1 \; or \; 2$)(-)
SF	Scaling factor (-)
$SF(t_e)$	Scaling factor dependent on t_e (-)
S_{front}	Saturation of phase 2 at the top of the saturation front (-)
S_{max}	Maximum saturation of phase 2 of the element nodes (-)
S_{min}	Minimum saturation of phase 2 of the element nodes (-)
S_{mid}	Middle saturation of phase 2 of the element nodes (-)

S_{res}	Residual saturation (-)
S_{tn}	Saturation at time step n (-)
S_{1r}, S_{2r}	Residual saturation of fluid phase 1 and 2 (-)
sv_{β}	Side vectors of the element in local coordinates
T	Thickness of an element (m)
${}_{2D}T_{3D}$	Transformation matrix from 3D global coordinates to 2D local coordinates
t	Time (s)
t_1, t_0	Indicates time step, 0 precedes 1
t_e	Time since the front entered an element (s)
Δt	Time step length (s)
V	Integration volume (m^3)
V^e	Element volume (m^3)
V^n	Mesh volume mapped to a node (m^3)
v_{α}	Advective velocity of fluid α (m/s)
x	Distance (m)
x_n	Normalised distance from origin (-)
x_{real}	Actual distance from origin (m)
x', y'	Local coordinate system
x_g, y_g, z_g	Global coordinate system
$\mathbf{u}$	Displacement tensor (m)
z	Height above datum (m)
α	Fluid phase (-), 1 or 2
β	Number from 1 to 3 unless otherwise stated
ϕ	Porosity (-)
μ	Dynamic viscosity (N/m^2s)
ρ_{α}	Density of phase α (kg/m^3)
ϖ_i	Weighting function of Galerkin Finite Element Scheme (-) for node i
ω_j	Weighting function of Galerkin Finite Element Scheme (-) for node j

$a_x, b_x, c_x, d_x, e_x, f_x, g_x$	Polynomial coefficients for a function $y = f(x)$
$a_s, b_s, c_s, d_s, e_s, f_s, g_s$	Polynomial coefficients for a function $y = f(S)$

1. Introduction

In this paper a hybrid analytical numerical approach for the modelling of two phase flow is presented. The application addressed is the forced replacement of hot brine in a caprock by supercritical CO_2 under reservoir conditions of temperature and pressure to be found at a depth of 1300 m. Modelling two phase flow using standard grid based numerical techniques presents a problem due to the sharpness of the front developed by the replacement of one fluid with another, balanced against the need to discretise the model into grid points and elements. One of the issues is that changes due to coupling to other processes, such as mechanical faulting and pressure release of the fluid, is likely to occur as the front passes. Depending on the resolution of the fluid flow grid, this time dependent signal may be missed or smeared with other signals loosing information on the integrity of the reservoir. In finite element approaches lower order based interpolation functions often fail to represent the sharp front and this can also lead to oscillations around the true solution. Finite volume methods can avoid these oscillations, but there are issues concerning the relative computational expense of these formulations and difficulties in representing smoothly varying heterogeneity fields while minimising discretisation overheads. Mixed finite element solutions whereby both the velocity field and the pressure solution are considered primary variables are finding some acceptance, however they are computationally more complicated to implement, especially with respect to solver capabilities, *Younes et al.* [2010].

Three main approaches have been adopted to address this problem. The most widely adopted approach is that of grid refinement, or adaptive mesh refinement in the vicinity of the front. The geometry of the grid is locally adapted to better represent the numerical processes operating at a local scale and represent steep gradients within the model. Recent examples for highly heterogeneous fields include *Chen, et al.*, [2003] and *Durlofsky, et al.*, [2007]. Such adaptive grid methods allow the discretisation scale to follow the front through the model, however the front location will always be approximated within the scale of the discretisation used. Such methods are extremely useful but can be computationally expensive and make coupling to other processes such as Thermal, Mechanical, reactive Chemical (TMC) more complicated due to the constant alteration in grid size and location.Interface tracking methods have been developed that apply sophisticated reconstruction algorithms based on either the ratio of volumes of a fluid in an element (Volume of Fluid Methods) or the advective velocity of the interface throughout the modelling regime (Level Set Method). *Meakin and Tartakovsky*, [2009], with references therein, review these approaches and conclude that there has actually been very little application of these techniques to multiphase fluid flow in fractured and porous media. Recent examples of their application include *Huang and Meakin*, [2008] and *Huang, et al.*, [2005]. *Unverdi and Tryggvason* [1992] followed the interface by explicitly representing the interface as a second grid moving through a stationary grid. *Glimm, et al.* [1999] tracked the front throughout the computational domain using a grid based interface reconstruction based on information in the grid element and the information from surrounding elements.

Interface tracking methods described above address the problem of the location of the front based on the volumetric fluid fluxes into and out of an element, the understanding that there must be continuity between elements and assumptions as to the shape of the front. The “front tracking” method developed in this paper uses a generic analytical solution to “add information” to the model and predict the location and shape of the front within the elements. This removes the necessity for adaptive mesh refinement and the need for further sophisticated reconstruction of the front surface. The information on the geometry of the front surface under the conditions given in the element is being predicted by the analytical solution. The method increases the accuracy of the prediction of the front location, but is still bound by the overall accuracy of the numerical method applied to determine the primary variables which the analytical solution depends upon. Examples of other hybrid analytical numerical methods where information is added to the model and thereby the computational load is reduced can be found in e.g. *McDermott, et al.*, [2007] and *McDermott, et al.*, [2009].

The method is developed within the object oriented, open source finite element code OpenGeoSys [www.opengeosys.net, *Wang et al.* 2009]. Although this Front Tracking method was specifically designed for the replacement of brine by supercritical CO_2 in a caprock under reservoir conditions, the generic nature of this approach is demonstrated.
The standard two phase flow equations are solved using the IMPES (implicit pressure explicit saturation) formulation (e.g. *Helming*, 1997). We formulate the saturation equation in terms of the volume of replacing fluid in the discretised elements. This volume may either be predicted using a standard first order approximation, or by using the analytical solution of the location of the front directly and integrating under this front. The latter approach works for homogenous conditions, and predicts radial flow better than the standard numerical methods using full upwinding schemes, however still requires further development for heterogeneous conditions. For clarity we will divide these approaches as follows

- FUG Full Upwinded Galerkin Finite Element Solution of the Pressure Equation
- FUG-v As 1 with a first order shape function approximation of the saturation equation (v stands for volumetric)
- FUG-a As 1 with the analytical solution used to derive the shape functions for the solution of the saturation equation (a stands for analytical)
- FUG-vT as 2 with the analytical solution and a volumetric reconstruction used to locate the front but not to evaluate the shape functions (T stands for front Tracking).

The emphasis of this paper is not the introduction of a new numerical method, but the combined use of a standard numerical techniques and analytical techniques. The analytical solution is used to introduce physical process understanding into the system, and to predict the location of the front at a sub-element scale based on both the fluid saturations present and the advective velocity field. Two key developments are shown

- The integration of an analytical solution in the finite element IMPES formulation to explicitly represent the shape and location of the saturation front
- The prediction of the location of the front in heterogeneous fields at a sub element scale.

2. Theory

Modelling of two phase flow in porous media can be described by the mass balance equations for each fluid phase and Darcy's law describing fluid flux under a pressure gradient (1).

$$S_\alpha \rho_\alpha \nabla \frac{\partial \mathbf{u}}{\partial t} + \frac{\partial (\phi S_\alpha \rho_\alpha)}{\partial t} + div(\rho_\alpha \mathbf{q}_\alpha) - \rho_\alpha Q_\alpha = 0 \qquad (1)$$

This equation includes poro-elastic deformation of the pore space, and changes in density of the fluid. The fluid velocity $\mathbf{q}_\alpha$ is a non-linear function of the pressure gradient, after Darcy's law

$$\mathbf{q}_\alpha = \phi S_\alpha \mathbf{v}_\alpha = \frac{Q_\alpha}{A} = -\frac{k_{r\alpha}\mathbf{k}}{\mu_\alpha}(\text{grad}\, p_\alpha - \rho_\alpha \mathbf{g}) \qquad (2)$$

Where $k_{r\alpha} = f(S_\alpha)$ given following. Here for the wetting phase (phase 1, brine in our example)

$$p_\alpha = p_w \qquad (3)$$

and for the non wetting phase (phase 2, CO_2 in our example)

$$p_\alpha = p_w + p_c \qquad (4)$$

here p_c is expressed as a negative suction pressure. *Helmig and Huber* [1998], discussed the solution of these equation systems using the Galerkin-type discetization Finite Element

Methods (FEM), and showed the limitations and advantages of the standard Galerkin approach, the Petrov-Galerkin method and the Fully Upwinded Galerkin (FUG) method. *Klieber and Riviere* [2006] presented work whereby several different Galerkin formulations were used creating a discontinuous Galerkin approach to model the two phase flow equations sequentially coupled with adaptive grid methods. *Hoteit and Firoozabadi* [2008], used a mixed finite element formulation and a discontinuous Galerkin approach to investigate the effects of capillarity on the flow system. They solved the saturation equation using fractional flow formulation and a total mobility approach. They showed that the permeability field as well as the effects of capillary entry pressure have a significant impact on the flow paths developed in two phase flow. From examination of equation (2) this is apparent, but it can also be seen that the effect of capillary entry pressure can be presented in the relative permeability function as a first approximation.

A full description of the finite element method may be found e.g. in [*Istok*, 1989; *Lewis and Schrefler*, 1998; *Zienkiewicz and Taylor*, 2005], and the finite volume method in *Versteeg and Malalasekera* [2007]. The hybrid analytical method presented here can be described as a multi scale approach [*Juanes and Patzek*, 2004]. The unknowns of the wetting phase pressure and the non wetting phase saturation are solved sequentially using different approaches. For the pressure formulation we apply the FUG (maximum mobility) approach, and for the solution of the saturation equation we introduce extra information in the model by including an analytical derivation of the shape function for the evaluation of the saturation front.

The advantage of using an analytical derivation for the location of the saturation front is that it removes the necessity to refine the mesh in the locality of the saturation front whilst still maintaining the sharpness of the front without numerical oscillations. The method, however, still has the requirement that the Courant time criteria apply for the advective flux of the front,[*Kolditz*, 2001], and, as is the case using a FUG scheme numerical diffusion is introduced. In addition the accuracy of the location of the front prediction is dependent on the accuracy of the numerical solution of the primary variables. It is true that mesh refinement can introduce a better representation of the field, but mesh refinement usually does not include further heterogeneity information, and therefore the accuracy of the prediction of the heterogeneity remains at the original grid scale [Thorenz et al. 2002].

To demonstrate the use of this hybrid method for the solution of (1) for two phase (liquid-liquid) flow and the prediction of the front we assume simplistic conditions. First that there is no pressure difference across the liquid-liquid phase fronts, i.e. capillary pressure effects are negligible, and that the solid-liquid-liquid contact angles have no significant impact on the flow characteristics. At a pore scale size it would be necessary to include these effects, discussed in detail by *Meakin and Tartakovsky*, [2009] and references therein. *Niessner and Hassanizadeh* [2008] examines the role of fluid-fluid interfaces and the impact they can have such as hysteresis. At the macro size, given the heterogeneity of geological medium (pore size distribution) and in this example the assumption of generally continuous fluid phases, these simplifications have some validity. Allowing this approximation means that the term p_c in (4) is neglected in the pressure formulation.

For the demonstration of the method we assume constant density and no deformation. This allows (1) to be expressed for a unit volume as (5) i.e. a volume balance equation

$$\phi \frac{\partial S_\alpha}{\partial t} - \mathrm{div}\left(\frac{k_{r\alpha}\mathbf{k}}{\mu_\alpha} \left(\mathrm{grad}\, p_\alpha - \rho_\alpha \mathbf{g} \right) \right) - Q_\alpha = 0 \qquad (5)$$

As $\sum_{0}^{phases-1} S_\alpha = 1$ in (6) by summing all the phases together we have

$$\sum_{1}^{phases}\left[\phi\frac{\partial S_\alpha}{\partial t}-\mathrm{div}\left(\frac{k_{r\alpha}\mathbf{k}}{\mu_\alpha}\left(\mathrm{grad}\,p_\alpha-\rho_\alpha\mathbf{g}\right)\right)-Q_\alpha\right]=0$$

$$\Downarrow \qquad (6)$$

$$\sum_{1}^{phases}\left[\mathrm{div}\left(\frac{k_{r\alpha}\mathbf{k}}{\mu_\alpha}\left(\mathrm{grad}\,p_\alpha-\rho_\alpha\mathbf{g}\right)\right)+Q_\alpha\right]=0$$

Consequently the governing equations for the two phases are turned into one parabolic and one Poisson equation as

$$\begin{aligned}&\phi\frac{\partial S_1}{\partial t}-\mathrm{div}\left(\frac{k_{r1}\mathbf{k}}{\mu_1}\left(\mathrm{grad}\,p_1-\rho_1\mathbf{g}\right)\right)-Q_1=0\\&\sum_{1}^{phases}\left[\mathrm{div}\left(\frac{k_{r1}\mathbf{k}}{\mu_1}\left(\mathrm{grad}\,p_1-\rho_1\mathbf{g}\right)\right)+Q_1\right]=0\end{aligned} \qquad (7)$$

Discretising the weak form of (7) into a grid with *np* grid nodes and *ne* elements, and integrating applying the Galerkin Finite Element method, we can write for the pressure field for all nodes, $i\in(0,\ldots,nodes-1)$ [*Thorenz* 2001], where the test function ϖ is the same as the shape function.

$$\begin{aligned}&\int_V\left(\phi\frac{\partial S_1}{\partial t}-\mathrm{div}\left(\frac{k_{r1}\mathbf{k}}{\mu_w}\left(\mathrm{grad}\,p_1-\rho_1\mathbf{g}\right)\right)-Q_1\right)\omega_i dV=0\\&\int_V\sum_{1}^{phase}\left[\mathrm{div}\left(\frac{k_{r1}\mathbf{k}}{\mu_1}\left(\mathrm{grad}\,p_1-\rho_1\mathbf{g}\right)\right)+Q_1\right]\omega_i dV=0\end{aligned} \qquad (8)$$

Solving this equation allows the derivation of (2) for all nodes. The saturation field for phase 2 and all nodes, $i\in(0,\ldots,nodes-1)$ is given by

$$\int_V\left(\phi\frac{\partial S_2}{\partial t}-\mathrm{div}\left(\frac{k_{r2}\mathbf{k}}{\mu_2}\left(\mathrm{grad}\,p_2-\rho_2\mathbf{g}\right)\right)-Q_2\right)\omega_i dV=0 \qquad (9)$$

After solution of equation (6) inserting (2), (9) can be rewritten for a unit volume as

$$\int_V\varphi\frac{\partial S_2}{\partial t}\omega_i dV=-\int_S\mathbf{q}_2\cdot\mathbf{n}\omega_i dS+\int_V Q_2\omega_i dV=f_2^i \qquad (10)$$

where the term $\int_S\mathbf{q}_2\cdot\mathbf{n}\omega_i dS$ is a surface integral and represents the sum of the fluxes of phase 2 into and out of the element across the surface S with a volume V. Expressing this in the discretised weak formulation and applying the Galerkin approach

$$\sum_{j\in N_i}\int_V\phi\omega_i\omega_j dV\frac{\partial\hat{S}_2^j}{\partial t}=f_2^i, i=1,2,\ldots,np \qquad (11)$$

where N_i denotes the set of nodes connected to node i, and $\hat{S}_w^j$ is the node value of the water saturation. Equation (11) forms a global system of equations where the number of equations corresponds to the number of grid points (np). This is expressed in matrix form as

$$\sum_{j\in N_i}C_{ij}\frac{\partial\hat{S}_2^j}{\partial t}=f_2^i \qquad i=1,2,\ldots,np \qquad (12)$$

where

$$C_{ij}=\int_V\phi\omega_i\omega_j dV \qquad (13)$$

Decomposition of the computational domain into finite elements means that the global matrices can be expressed as

$$C_{ij} = \sum_{1}^{ne} C_{ij}^{e} \tag{14}$$

$$f_{2i} = \sum_{1}^{ne} f_{2i}^{e} \tag{15}$$

This forms what we will refer to as the standard FUG-FE approach.

However, to be able to include analytical solutions predicting the geometry of the saturation front we use the solution of (10) derived from the pressure equation to calculate the flux into or out of an element, and integrate with respect to time to explicitly include the actual volume of CO_2 (phase 2) change in an element. The total amount of phase 2 present can then be expressed in volumetric terms using *t* to represent the time step of evaluation as

$$V_2^{n(t_1)} = V_2^{n(t_0)} + f_2\left(t_1 - t_0\right) \tag{16}$$

were V^n represents the finite volume of the modelling area represented by a node surrounded by *ne* elements, each attached element with *nn* nodes, where V^e represents the volumes of the elements surrounding the node.

$$V^n = \frac{\sum_{e=1}^{ne} V^e / nn}{ne} \tag{17}$$

To relate (16) to the saturation of a phase we use

$$V_2 = S_2 V^n \tag{18}$$

which leads to (16) being expressed at an element level as

$$\phi V^n \int_{S_2^{(t0)}}^{S_2^{(t_1)}} \partial S_2 = f_2 \int_{t_0}^{t_1} \partial t \tag{19}$$

Using a finite difference formulation (19) can be solved explicitly for $S_\alpha^{(t_1)}$ as

$$S_2^{(t_1)} = \frac{\left(\phi V^n S_2^{(t_0)} + f_2 \Delta t\right)}{\phi V^n} \tag{20}$$

Again the above equation (20) forms a global system of equations where the number of equations corresponds to the number of nodes, or grid points.

The evaluation of $\mathbf{q}_2$ (2), and therefore f_2 explicitly by the finite element method has the advantage of including the off-diagonal components in the evaluation of the flow vector, but the disadvantage that local mass conservation is not always adhered to, both in contrast to the standard box finite volume approach. Prior to introducing a more rigorous method of calculating fluxes at the nodes, we include a term to remove the effects of local mass imbalances. This term can be seen as an enhanced numerical dispersion term, but has the advantage in coupled process modelling that the solution is stable without oscillations. To correct for this missing local mass balance information, after solution of the saturation equation, the saturation at all the nodes is checked to ensure all are equal to or above the residual saturation value within a defined tolerance level. Where nodes are found where saturation is below the residual value, then mass from the surrounding, now “donating” nodes, weighted by these donating nodes saturation above the residual saturation, is taken and added to the “offending” node to reach residual saturation. By this means the overall mass balance is not impaired and a satisfactory saturation solution is obtained.

The term $V^n \phi S_2^{(t_0)}$ represents the volume of the replacing fluid at the previous time step. Using a linear interpolation (FUG-v approach) this can be represented as the sum by the number of nodes (nn) of the product of the saturations multiplied by the volume represented by that node in the element. Here *T* is the thickness of the element and A_{ne} is the planar area represented by the node in an element.

$$V^n \phi S_2^{(t_0)} = T\phi \sum_1^{ne} S_2 A_{ne} \qquad (21)$$

The analytical solution for the presence of the front within the element provides the location of the front both according to the saturations at the nodes in the element and the advective flow velocity and direction. In the FUG-a approach (21) is replaced as

$$V^n \phi S_2^{(t_0)} = \phi \sum_1^{ne} \int_\Omega \Phi d\Omega \qquad (22)$$

Where $\int_\Omega \Phi d\Omega$ represents the integration of the predicted saturation surface of the analytical solution Φ where $\Phi = f(v_x, v_y, v_z, S_{2\,n=1..nn})$ in the volume Ω being that space in an element occupied by part of the saturation surface.

The analytical solution can be used to both evaluate the location of the saturation front and to calculate the volume of the replacing fluid around a particular node. What we call the FUG-vT approach is where we use (21) for the solution of two phase flow with the analytical solution $\Phi = f(v_x, v_y, v_z, S_{2\,n=1..nn})$ to predict the actual location of the front within elements. We note here, discussed later, that there are some locations where there is not a unique solution for the analytical approach. Und under these conditions we use a volumetric reconstruction method.

2. Front Tracking

2.1 Choice of analytical solution

To be able to evaluate the volume of the replacing fluid, the volume underneath the saturation surface needs to be calculated. Triangular elements offer the possibility of representing a global three dimensional flow field (q_x, q_y, q_z) in two dimensions in the local coordinate system of the elements [Kolditz 1995]. This method has been used several times for instance for fracture network simulations, e.g. *McDermott, et al.* [2006] as well as standard 2D cross sections. In addition it is often standard practice to represent large scale aquifers as 2D bodies with a certain thickness. Unique to triangular elements is the possibility to further reduce this two dimensional flow field uniquely to one dimensional flow representative of the entire element using a standard three point approach. In this manner the flow in the element is reduced to a one dimensional flow field, within the coordinate system *x,y,z*. Different analytical solutions can be considered for determining the location of the two phase flow front, in this work for the demonstration of the method we apply the original 1D solution derived by *Buckley and Leverett* [1941] for the replacement of one fluid with another in two phase flow. This solution is developed for equilateral triangular elements as these are geometrically simplest for the integration of the volumes of the elements.
The *Buckley and Leverett* solution is one of the simplest for two phase flow where capillary pressures are not considered to be causing any resistance to flow. We discussed earlier our

reasoning behind this as a first approximation leaving out the capillary pressure term in our evaluation of the pressure field. The capillary pressures is, however, included indirectly in terms of allowing residual trapping by the consideration of a residual saturation for the calculation of the relative permeability functions below. There are several publications where the capillary pressure term is included, and it would be possible also to include a more sophisticated solution for front tracking e.g. *Chen* [1988], *Fucik, et al.*, [2008], *McWhorter and Sunada* [1990] *van Duijn and de Neef* [1998]. *Buckley and Leverett* [1941] used relative permeabilities described by the functions given below (23) derived from their laboratory work. Presentation of more complex constitutive relationships can be found e.g. in [*Brooks and Corey*, 1964; *Helmig*, 1997; *Helmig, et al.*, 2002; *Ippisch, et al.*, 2006; *van Genuchten*, 1980].

$$k_{r1} = \frac{(S_1 - S_{1r})^2}{(1 - S_{1r} - S_{1r})^2} \quad \text{and} \quad k_{r2} = \frac{(1 - S_1 - S_{2r})^2}{(1 - S_{1r} - S_{2r})^2} \tag{23}$$

The *Buckley and Leverett* analytical solution of the saturation equation considering fractional flow functions is presented by *Thorenz* et al. [2002] as being

$$\Delta x = -\frac{q_{total}}{\phi} \frac{\partial \left(\frac{1}{1 + \frac{k_{r2}\mu_1}{\mu_2 k_{r1}}} \right)}{\partial S} \Delta t \tag{24}$$

From this equation it is possible to derive the saturation curve presented in Figure 1. Helmig (1997) presents two methods of solving this equation. The equation (24) has two possible saturations for one location. Using the equal area solution the actual location of the saturation front is determined by constructing a shock front whereby “Area 1” is equal to “Area 2”.

2.2 Locating the saturation front

In Figure 1, the solution of the *Buckley and Leverett* equation has been normalised against the maximum distance md from the origin for the extension of the saturation front. Examining (24) it can be seen that the term $\frac{q_{total}}{\phi}\Delta t$ is a scaling term, and for the solution presented in Figure 1 we set this to 1.

This means that it is possible for any combination of flow rates, porosity and time to be compared with the normalised analytical solution via a scaling factor. This fact is central to the application of this analytical solution.

The shape of the analytical solution from the origin to the saturation front can be approximated by a polynomial (25) fitted to match the normalised analytical response (Figure 2). Therefore a standard response for the solution assuming constant material permeabilities and viscosities within an element may be evaluated by solving (24)

$$x_n = a_s S_2^{\,6} + b_s S_2^{\,5} + c_s S_2^{\,4} + d_s S_2^{\,3} + e_s S_2^{\,2} + f_s S_2 + g_s \quad \text{i.e. } x_n = f(S_2) \tag{25}$$

The coefficients $a_x \ldots g_x$ are the fitted polynomial coefficients for the normalised distance approximation. To calculate profile under operating conditions we can now apply

$$x_n = \frac{x_{real}}{\left(\frac{q_{total}}{\phi} \Delta t \bullet md \right)} \tag{26}$$

For simplicity we define a scaling factor term so that

$$SF = \frac{q_{total}}{n} \Delta t \bullet md \quad (27)$$

Therefore the location of the saturation front from an origin given the flow, porosity and time conditions in the scaling factor is given as

$$x_{real} = x_n \bullet SF \quad (28)$$

Likewise we define the inverse polynomial function so that

$$S_2 = a_x x_n^{\,6} + b_x x_n^{\,5} + c_x x_n^{\,4} + d_x x_n^{\,3} + e_x x_n^{\,2} + f_x x_n + g_x \quad \text{i.e. } S_2 = f(x_n) \quad (29)$$

with $a_s \ldots g_s$ being the polynomial coefficients for the saturation approximation.

These approximations allow for the calculation of either the distance to the front from a known saturation (25) or the saturation at a known distance (29).

2.3 Implementing the analytical solution information

To demonstrate the ease of the implementation of this approach for the user, as an example the required input code for OpenGeoSys to trigger the HAN approach is presented in Figure 3. Four extra lines of text are required in the numerical description. The lines marked ";" being commented out and for description. The lines marked with "$" acting as triggers for the reading of the code, the numerical values referring to values and coefficients required in the analytical solution. The polynomial coefficients, equations (25) and (29), the scaling factor (27) and the front saturation are derived by fitting of the analytical solution using an external program, in this case Excel. The values of residual saturation and maximum saturation are defined by the constitutive relationships used for the calculation of relative permeability.

2.4 The front in triangular elements

At any particular time during the solution of (9) the value of saturation of the three nodes in the triangular element is known. These nodal values for phase 2 are defined as S_{max}, S_{mid} and S_{min} being the maximum, middle and minimum values respectively. S_{front} is the saturation front calculated from the analytical solution and S_{res} is the residual saturation of the phase 2. Depending on the saturation values of the nodes, the saturation front may be

- Present within the element
- Have passed through the element
- Not have reached the element.

Each of these cases are now studied consecutively in detail. In each case we determine a volume (m^3) in the element to be filled by the incoming saturating fluid phase 2. For all cases the volume available to the incoming fluid is calculated for an element of unit height. To include non-unit element height, e.g. fracture aperture, the element storage matrix can be scaled with the given element height.

2.4.1 The front is present within the element

Figure 4 and Figure 5 illustrate the two cases when the front has entered the triangle element. In one or two nodes the saturation values are above S_{front}. The location of the saturation front in an element is determined as a distance from a fixed point, and the surface integrated within the local element coordinates to give the volume available for the incoming saturating fluid to occupy.

The element global coordinate (x_g, y_g, z_g) system is transferred into a local coordinate system (x', y') whereby the node with S_{max} is located at the origin (0,0).

$$\left[A'_{2D}\right] = \left[A^g_{3D} - P_{S\max}\right]\left[{}_{2D}T_{3D}\right] \tag{30}$$

$$\left[{}_{2D}T_{3D}\right] = \begin{bmatrix} \cos(x', x_g) & \cos(y', x_g) \\ \cos(x', y_g) & \cos(y', y_g) \\ \cos(x', z_g) & \cos(y', z_g) \end{bmatrix} \tag{31}$$

Locating S_{max} with the origin in the local coordinate system provides a fixed point from which to calculate the location of the front. The velocity vector is also transformed such that

$$\mathbf{q}' = \sum_{1}^{phases} \mathbf{q}_\alpha \left[{}_{2D}T_{3D}\right] \tag{32}$$

The scaling factor SF (27) of the element is now calculated from the porosity, the flow velocity, and the time passed since the front entered the element t_e. Allowing D_{node} and D_{front} to be the distance of the front to the origin of the two phase flow difference $D = D_{front} - D_{node}$ represents the downstream distance of the front from the node in the element. In the case where two nodes have a higher concentration than the saturation front then two distances are calculated. D_{front} is the normal distance from the node to the front. It can be shown that for a length of time t_e since the front has entered the element that the distance between the saturation front and the node with a saturation S_{max} $\left(D1_{front}\right)$, and in the case where Smid > Sfront, (also for this node with saturation S_{mid} $\left(D2_{front}\right)$) is :-

$$\begin{aligned} D1_{front} &= SF\left(t_e\right)\bullet\left(f(S_{front}) - f(S_{max})\right) \\ D2_{front} &= SF\left(t_e\right)\bullet\left(f(S_{front}) - f(S_{mid})\right) \end{aligned} \tag{33}$$

The time t_e is the difference between the current time step and the time when the front is recorded at having first entered the element, marked by the saturation concentration of the node first exceeding the front saturation $S_{front} / 2.0$.

Now that the distance of the saturation front to the nodes is known, the volume under the saturation surface is evaluated and allotted to the nodes in the triangular element to define the element matrix C^e_{ij}, such that

$$C^e_{ij} = \phi \begin{bmatrix} MN1 & 0 & 0 \\ 0 & MN2 & 0 \\ 0 & 0 & MN3 \end{bmatrix} \tag{34}$$

Where the individual sum for each node is then

$$V_i^n \phi S_2^{(t_0)} = \sum_{1}^{ne} C_{jk} \text{ where i=j=k } C_{jk} = MN, \text{ else } C_{jk} = 0 \tag{35}$$

MN represents the volume of replacing fluid in the element. In (34) we have assumed that the nodes in the triangular element are ordered S_{max}, S_{mid} and S_{min}, naturally this may be different. For ease we have defined MN1 as the volume to be attributed to the node with the maximum saturation, down to MN3 with the lowest saturation.

For the case that volume of replacing fluid within an element is to be calculated using the analytical solution, the location of the front within the element is located as described above, and the polynomial expression describing the shape of the front integrated to provide the volume. Local geometrical considerations need to be taken into account. The implementation can be time consuming.

2.4.2 The front has passed through the element

In this section we consider the case where the saturation front has passed the element completely. This means that the saturation of all the nodes is higher than the front saturation. For this scenario we use for a first order linear approximation of the volume of replacing fluid. Here

$$C_{ij}^{e} = \frac{\phi A}{nn}\begin{bmatrix} MN1 & 0 & 0 \\ 0 & MN2 & 0 \\ 0 & 0 & MN3 \end{bmatrix} \tag{36}$$

Where

$$\begin{aligned} MN1 &= Smax \\ MN2 &= Smid \\ MN3 &= Smin \end{aligned} \tag{37}$$

Only where the saturation front is strongly curved is it of conceivable advantage to include a function integrating under the surface to determine more the volume more accurately. The implementation is time consuming and from experience the extra accuracy brings little advantage.

2.4.3 The front has not yet reached the element

The last case is if the replacing fluid has not yet entered the element, i.e. $S_{front} > S_{max}$ and S_{mid} and S_{min}. For this case we apply (36) and (37) as above.

2.4.4 Boundary conditions

For the solution of (6) for the pressure throughout the system, a pressure boundary condition and initial condition are necessary. Examining the saturation equation (9) it can be seen that all the entries in this equation system are flux entries. The boundary integrals need to represent the flux into or out of the model area. Where the boundary integrals are directly entered in the modelling as source terms or pressure dependent source terms in the input commands this is accounted for. However where there is no specification, to ensure a stable solution of the equation the boundary integrals need to be included in the evaluation of the equation. In practice an “Open boundary” is identified, and when the saturation front arrives at this boundary, the flux entering the boundary element, i.e. an element with a node on the boundary, is used to specify a source term on the open boundary. If the total flux entering the boundary element equals the sum of the source terms removing the flux from the element representing the open boundary then the saturation front never reaches the boundary, being always removed before it gets there. In the present work we use a gradient approach based on the saturation of the nodes. The average saturation of the nodes in an element on the boundary $S_{\alpha b}$ or on the inner side of the model, S_{wi} is given by

$$S_{2b} = \frac{\sum_{0}^{nb} S_2}{nb}, \quad S_{2i} = \frac{\sum_{0}^{ni} S_2}{ni} \tag{38}$$

Where nb and ni represent the number of nodes on the boundary or inside the model respectively of the element in question. The saturation is linearly interpreted and added to the boundary saturations to interpret the next time steps saturation such that

$$S_{2b\,t_1} = \frac{S_{2i\,t_0} - S_{2b\,t_0}}{2} + S_{2b\,t_0} \tag{39}$$

where t_1, t_0 represent time steps

These values of saturation are substituted in to the current solution for saturation, and the boundary integrals (fluxes) for the next time step are evaluated

$$f_{2i} = C_{ij} S_{2i} \qquad (40)$$

2.4.5 Adaptive time step control

For the front to be effectively tracked through the elements, it is necessary to ensure that no time step is so large as to cause the front to pass right across the area represented by a node in an element in one time step. As the saturation of the elements in the model area increases, so the relative permeability increases, and so the fluid velocity increases. We have not observed a control on the lower end of the time step, i.e. it can be small without causing numerical problems. However for a time efficient solution, the time step needs to be as large as possible without compromising the model accuracy. The velocity of the saturating phase can be calculated throughout the model area after each time step, and the time step adjusted to ensure that the Courant stability criterion for ½ of the element length is not exceeded.

2.4.6 Discussion of the method and application

The grid based FUG finite element solution provides nodal values of flux. The method includes numerical dispersion induced by fully upwinding which prevents oscillation around the sharp front, (Helmig 1997). This can be seen as a tendency for the front to diffuse downstream from its actual location, the mass thereof being taken from upstream of the front. Without going into more complicated methods of reconstructing the front this seems to be a necessary penalty for using the FUG method. The values of flux and saturation in the grid based approach represent the best approximation for a smooth solution of the balance equations. The saturation equation is, however, not continuous, and therefore the value for the saturation in the vicinity of the front is averaged out. This is best understood by considering a front passing through a node. Only when the front has passed through the node and completely filled the volume assigned to that node will the saturation of that node be calculated as of at least the front value. Whilst the front is still within the refines of the node, the average saturation of the node will be less than the front. This created a problem for a method which relies on the knowledge of the saturation of the node as a pin point value, and leads to a numerical smearing of the approach by the length of one element. For the case where we use the analytical solution to find the location of the front (FUG-vT) the search criteria can be attuned to this issue by taking into account this smearing, enabling the analytical solution to identify the correct location of the front. However, so far in the case that we want to use the analytical solution to determine the volume of CO_2 present exactly at the front where this smearing occurs, we have only achieved partial success (FUG-a) .

A further problem arises due to the combination of the analytical solution and the FUG approach. When a front is passing through an element the FUG approach assigns flux to the downstream nodes, even although the front has not yet reached that node. Within the analytical solution there is no information for saturations between the front saturation and residual saturation. According to the analytical solution they do not exist. Using only the analytical solution as the basis function to define the volume of replacing fluid will lead to incorrect assumptions about the fluxes at the element boundaries. For the homogeneous case this can be corrected by considering the flow direction, and the amount of missing mass and scaling accordingly. However in the heterogeneous case it has not been possible yet to get a stable satisfactory solution. The FUG-v approach does not have this problem.

We demonstrate the use of the analytical solution alone (FUG-a) for homogeneous cases, and then the FUG-vT for the determination of the location of the front in heterogeneous systems. Where no solution from the analytical approach exists for the location of the front, we apply a volume correction method to predict its location. That is the mass is redistributed within the element so that a front with the appropriate saturation can be constructed whist still adhering to the volume predicted by the saturations at the nodes.

3. Model Validation and Application

The main aim of this modelling development is to aid in the understanding of coupled processes operating during the injection of supercritical CO_2 beneath a caprock and the breakthrough of this CO_2. In addition we want to identify the location of the front at a scale smaller than the element discetisation we are using and be able to apply this information computationally efficiently coupled to other processes. To demonstrate the modelling approach, the fluid properties of the supercritical CO_2 and brine were selected to represent conditions at a depth of approximately 1300 m below the ground surface. A pressure of 130 bar was chosen and a temperature of 40 °C. Five models are presented with increasing degrees of complexity.

1) Initially a comparison is made between the simplified 1D analytical solution for two phase flow by *Buckley and Leverett* [1941], the FUG-a and FUG-v scheme and show the prediction of the location of the front using the FUG-vT approach.
2) Secondly a model of the caprock is considered with supercritical CO_2 injection and heterogeneity in the permeability field.
3) The radial injection of CO_2 into a homogeneous field is considered
4) Injection to the base of a caprock is considered with a randomly distributed heterogeneous permeability field.
5) Finally the method is compared to a standard finite volume simulation of a heterogeneous field using a finite volume rendition of the triangular finite element grid.

3.1 Model 1: Analytical, numerical and hybrid model comparison

Comparison of the purely analytical, purely numerical FUG-a, FUG-v and FUG-vT approaches is based on the caprock application, illustrated in Figure 8. At the base of the caprock supercritical CO_2 pooling is represented by source terms providing circa 1.67 litre/day. The results presented in Figure 8 are for the distribution of the CO_2 after 42.6 days of injection. There is a pressure control on the upper boundary, ensuring that when the supercritical CO_2 breaks through the upper boundary it is free to escape, and no pressure control on the lower boundary, meaning with increased rate of injection there is an increase in pressure on the lower boundary. The upper boundary is defined as an open boundary for the saturation equation. As the injection of supercritical CO_2 is source term driven rather than pressure driven, until the CO_2 finds a pathway through the caprock, pressure at the injection boundary increases. Once a pathway starts to develop towards the upper boundary so the significant flows of CO_2 can occur as the fluid is no longer required to displace large volumes of brine, hence the pressure reduces. A capillary entry pressure term would increase the amount of pressure required to be built up in the system prior to the CO_2 creating its escape path.
The fluid and material properties for this model are presented in table I & II respectively. The relative permeability functions assumed are those from *Buckley and Leverett* [1941], and illustrated in Figure 9.
A comparison in profile with the *Buckley and Leverett* analytical solution is provided in Figure 10. Here FUG method for the solution of the pressure equation is presented coupled with the

three different approximations of the solution of the saturation equation (FUG-v, FUG-a, FUG-vT). First the standard linear interpolation, secondly using the volume predicted by the analytical function, and thirdly again using the volume predicted by the analytical function, but redistributing mass to upstream nodes to allow for the mass correction, i.e. accounting for the saturations between the front saturation and residual saturation which the analytical solution suggests does not exist and is a product of the FUG scheme. All three schemes can be seen to approximate the purely analytical solution. It is interesting to note that all three approaches produce similar results.
When identifying the location of the front (FUG-vT), what is striking is that the combination of the FUG-v scheme using the standard linear interpolation coupled with the analytical method for the prediction of the location of the saturation front yields a result which is almost exactly the pure analytical result, illustrated as “Location of front tracking estimate”. This result suggests that the FUG-vT combination can be relied upon to produce accurate predictions of where the front is likely to be provided a solution to the analytical formulation exists.

3.2 Model 2: Well injection in a homogeneous media

By definition upwinding schemes propagate downstream information in elements instantaneously upstream to the front. This prevents information downstream (infront of) of a propagating front from impacting the movement of fluid which is controlled only by upstream (behind the front) information. The disadvantage of this useful approach is that as soon as fluid enters an element, the entire element gets the upstream flow characteristics, and therefore the numerical dispersion caused by this approach propagates in the shape of the elements through the grid. The evaluation of the saturations in this case is based only on the flux at each node. As the evaluation of the saturation surface in the FUG-a case is based upon the predicted saturations and the flow field, some shape correction due to the flow field contribution can be expected. This correction can be to the degree that the propagation from a point source becomes circular, as demonstrated in Figure 11, the parameters being the same as model 1.

3.3 Model 3: Single band of low permeability material in higher permeable field.

In this model we repeat the scenario described in model 1, except we introduce a low permeability band just above the injection area (see Table II for parameters). Fluid flow is forced around this band, the performance of the purely numerical FUG-FE scheme and the hybrid FUG-vT models are compared in Figure 12. The numerical model is no longer able to cope with the heterogeneity in permeabilities. It can no longer satisfactorily represent the saturation front, and the linear averaging technique in the volumetric averaging leads to oscillation in the solution below the residual saturation (20%) and above the maximum saturation (80%). The FUG-vT hybrid model copes well with the heterogeneity, the reduction in the minimum saturation to 19.5% is within the tolerance written into the model code. The solution time for the FUG-vT approach is approximately ½ that of the standard FUG finite element numerical approach. In addition we note that the front prediction is reasonable. The disjointed nature of the front comes from the fact that information from the flow field and the saturations is used to form the front location prediction and where the analytical solution can not predict the location of the front, a volume interpretation approach is used. In addition the graphic program used to shade the regions utilises a linear approximation for shading, which is not always appropriate.

3.4 Model 4: Application to a heterogeneous cap rock

Here we again repeat the scenario described in model 1, except we now introduce three orders of magnitude of random heterogeneity (Table III). In this model we introduce the time step control discussed above.
The FUG numerical model without grid adaptation can no longer come to a reasonable solution of the model. After a model total time of circa 50 days had been reached, the solution showed a maximum saturation of 102% and a minimum saturation of -40%. In comparison the FUG-vT approach after 1000 time steps had reached a model time of circa 75 days, required less real time to reach this solution and showed no oscillation on the saturation solution, i.e. a maximum saturation of 80% and a minimum of 20%. Figure 13 presents the results of the FUG-vT method for the injection into the caprock represented by a heterogeneous field of permeabilities. The solution is stable between 20% saturation and 80% saturation. In addition the front location is also demonstrated to be reasonable.

3.5 Model 5: Well injection in a heterogeneous media

The FUG-vT approach is now used to simulate injection of supercritical CO_2 into a layer which can be taken as underlying a caprock. The CO_2 spreads out laterally from the injection point, and forms channels as a result of the heterogeneity (see Table III). This is demonstrated in

Figure 14, here again the front tracking can be seen to be providing sub element scale information the location of the saturation front. As the most significant changes in coupled processes will occur at the location of the front this information is important. Although exact heterogeneity of the subsurface is unlikely to be known, the general distribution of heterogeneity will be known. Therefore is it important to be able to predict the density and general distribution of the channels in the subsurface to be able to relate them to other processes, such as seismic signals due to mechanical coupling. In Figure 15 we compare a larger area subject to well injection, and again the models are scalable, so what is of relevance is the density of the mesh elements and the heterogeneity they represent.

In Figure 15 we also compare the results of a finite volume approach utilising an identical physical model and the FUG-vT method presented here. In this figure the front tracking location is presented, then removed for comparison to the finite volume (FV) approach. The FV calculation was implemented in the Quintessa Ltd multi-physics code QPAC (www.quintessa.org/qpac), adopting the same element structure for the finite volume grid. The two codes had previously been successfully cross-compared using Models 1 and 3 discussed above. We note that the overall shape of the predicted radial flow patterns is similar, and many features can be cross referenced. The FUG-vT method predicts the formation of more discrete and higher saturated channels, the FV scheme predicts more distribution in the saturating phase. This is due in part to the differences in the numerical schemes, specifically concerning the tendency for the finite element approach to 'blur' permeability contrasts across elements as the fluxes are assigned to the nodes by integrating across the elements. This creates the possibility for channelled pathways that the finite volume approach would not include. Previous experience has indicated that grid convergence exercises simply sub-dividing the existing triangular elements (and hence keeping the heterogeneity pattern identical) would yield further convergence of results.

Particularly the FUG-vT prediction would suggest that should micro seismics occur as a result of the injection of CO_2 that the signals would be more localised to the channel locations, and that they would also not be confined to a radial distribution at the outer edges of the injection plume. However we also note that given the uncertainty in the prediction of the subsurface heterogeneity that both methods provide a valid approach to identifying the general spread of CO_2.

Strictly speaking the FUG-vT model does not allow capillary trapping to occur, although the pattern of flow predicted by the results would suggest this. The flow in the system is driven by the source term representing the well and pressure field developed by the well. Preferential flow as a consequence of the heterogeneous permeability field leads to the partial isolation of low permeability blocks within the flow system. This is exaggerated by the positive feedback caused by the relative permeability functions, i.e. the higher the saturation, the higher the permeability. Should capillary pressure also be included in the calculation, these low permeability areas would be even more sealed from the preferential flow channels.

3.6 Application & scaling of model results

In the scenarios selected, the rate of flow through the heterogeneous media is controlled by the source term injecting the fluid. The fluid pushed into the domain must escape at the other end or side of the model. This dictates the rate of breakthrough, and to that end the pressure will build up until the breakthrough occurs. The pressure solution is a reflection of (slave to) the rate of fluid entry into the system and the permeability of the system.

To illustrate this more clearly, one could write the standard Darcy equation where the term Q represents the flow rate through the whole model (m^3/s), A represents the cross sectional area of the model (m^2), $\frac{k}{\mu}$ the ease at which fluid flows through the whole model system ($m^2 / Pa\,s$), sometimes called mobility, and i the pressure gradient across the model (Pa/m) see (41).

$$Q = A\frac{k}{\mu}i, \qquad (41)$$

Keeping A and $\frac{k}{\mu}$ constant means that $Q \propto i$. Likewise if Q is kept constant, and only k is altered, as perhaps would be the case in fitting the permeability to different caprock values, then the pressure gradient i would change. An example would be a situation where the predicted entry of supercritical CO_2 into the caprock is $1/10^{th}$ of the rate modeled, and the permeability of the caprock two orders of magnitude less than used here. The time required for

breakthrough would then be 10 times longer than given here, and the pressure build up two orders of magnitude greater.
Applying this concept to reality for a system with a heterogeneous permeability from 1 mD to 0.001 mD (i.e. $1\times10^{-15}m^2$ to $1\times10^{-18}m^2$) the pressure build up would be of the order of 0.6 MPa. The entry pressure of the CO_2 into the caprock would also impact the pressure build up, but the effect would be that of reducing the permeability until the capillary pressure had been overcome. Increasing the thickness of the caprock linearly decreases the pressure gradient, but as the pressure gradient does not control the flow in this system, rather the amount of CO_2 entering the base of the caprock, this will only have a significant impact where the pressure gradient falls below the capillary entry pressure. For a system described above where the capillary entry pressure is not considered, doubling the thickness of the caprock will double the time required for breakthrough to occur.
The scenario presented in 3.5 clearly suggests that in a heterogeneous system that the spread of CO_2 is dominated by channel flow. This is logical, as the saturation relative permeability relationship provides a positive feed back mechanism, i.e. the more saturation, the higher the permeability and vice-versa until full saturation is reached. The consequences of channelling in the reservoir will be to localise the impact of the injected CO_2.

4. Conclusions

In this paper we have presented a new hybrid analytical numerical method for modelling two phase flow through heterogeneous porous media and locating the saturation front. This method uses a generic analytical solution of two phase flow though porous media to add extra information into a standard Galerkin Finite Element numerical procedure for solving two phase flow. The advantage this technique brings is that it removes the necessity of adaptive mesh refinement in the vicinity of the shock front generated by two phase flow replacement, to capture the location of the front. The front location is tracked as it passes through the triangular elements, this information can be passed onto other coupled processes. The fluid pressure in the area to be modelled is solved using a Fully Upwinded Galerkin (FUG) approach. The saturation equation is reformulated so that the shape functions represent the volume under the two phase flow surface available to the incoming saturating fluid. The volume in elements where the front is present is given both by applying the analytical solution under the flow conditions found in the element being considered and using a linear averaging approach.
Under homogeneous conditions the calculation of the distribution of the saturating fluid in the elements using the analytical function can be used to satisfactorily solve the saturation equation, provided that the area where the analytical solution provides no values of saturation for (at the shock front) is taken into account. As the analytical function combines information on both the element saturations and on the flow field in an element, it is able to represent radial injection in a homogeneous system better than a fully upwinded system. For more complex heterogeneous flow fields further development would be required to develop better flux transfer functions across the elements. However the information within the element can still be used satisfactory to predict the location of the front at a sub element scale, information which is important when considering heterogeneous flow fields and the scale of modelling.
The modelling work was developed to consider the replacement of brine by supercritical CO_2 in a both virtual caprock under conditions of pressure and temperature equivalent to a burial depth of 1300m, and a reservoir rock under the same conditions of temperature and pressure. The development was carried out in the open source code Open GeoSys.
For verification the methods are compared against a standard analytical solution for two phase flow, the standard FUG-Finite Element (FUG-FE) numerical scheme with volume averaging for the saturation equation and a Finite Volume model for heterogeneous permeability distribution. The standard FUG-FE scheme was not able to cope sufficiently with the heterogeneities without grid refinement, and quickly started to predict saturations below the residual saturation of above the maximum saturations of the fluid in the system. However the FUG-vT approach could deal with the heterogeneities without grid refinement, the saturation profiles it predicted

were smooth and within the residual and maximum saturations for the fluid in the system. In all cases the FUG-vT approach required significantly less time than the standard FUG FE approach to come to a stable solution.
In the modelling comparison it was shown that the results are scalable depending on pressure, permeability and the volume applied by the source term. This model as it stands can be used to make an initial assessment of caprock integrity during CO_2 injection and the potential pattern of lateral migration of CO_2 in a reservoir.
Removing the requirement for grid refinement and providing a stable solution to the flow equations creates a stable basis for the further consideration of coupled processes, such as heat transport, reactive mass transport and mechanics on the same grid scale.
Beyond the current application, the Front Tracking FUG-vT method whereby an analytical solution is integrated into the numerical formulation to add physical information to the model provides a new approach to modelling other two phase flow systems, for instance hydrocarbon systems. The approach is not confined purely to the reservoir conditions chosen, it is a simple matter to apply different fluid and material properties derived from other constitutional relationships reflecting different temperatures, pressures, fluids and models of relative permeability.
Introduction of different analytical solutions in the model to predict the volumes of the fluids is possible adding extra information, thereby reflecting conditions and processes to be investigated more accurately, for instance further work in this area includes the addition of the analytical solution for two phase flow under the influence of capillary entry pressure. Further work could also include coupling the scheme to higher order estimates of the pressure and velocity field in heterogeneous conditions ensuring that the local as well as global mass balance is better adhered to.
Finally we note that the injection of supercritical CO_2 into a reservoir rock will be strongly influenced by the heterogeneities present and the development of viscous fingering. It seems that it is over simplistic to assume a radial spread of CO_2 from the well centre. Monitoring for the front of a radial plume may loose a lot of the important details in the mechanics of the spread and distribution of the real CO_2 plume. A front tracking method may help to better identify the coupled processes operating and methods of managing CO_2 migration.

Acknowledgements

The research leading to these results has received funding from the European Community's Seventh framework Programme FP7/2007-2013 under the grant agreement No. 227286 as part of the MUSTANG project and from the Scottish Funding Council for the Joint Research Institute with the Heriot-Watt University which is part of the Edinburgh Research Partnership in Engineering and mathematics (ERPem).

References

Brooks, R. H., and A. T. Corey, Hydraulic Properties of Porous Media., *Hydrol. Pap.*, *3*, Band 3, Colorado State University, Fort Collins, (1964).

Buckley, S. E., and M. C. Leverett, Mechanism of Fluid Displacements in Sands, *Transactions of the American Institute of Mining and Metallugical Engineers (TAIME)*, *146*, 107-116, (1941).

Chen, Y., L. J. Durlofsky, M. Gerritsen, and X. H. Wen, A coupled local-global upscaling approach for simulating flow in highly heterogeneous formations., *Advances in Water Resources*, *26*, 1041-1060, (2003).

Chen Z, X. Some invariant solutions to two-phase fluid displacement problems including capillary effect, Soc. Pet. Eng. Reservoir, Eng., 3(2), 691-700, (1988).

Durlofsky, L. J., Y. Efendiev, and V. Ginting, An adaptive local-global multiscale finite volume element method for two-phase flow simulations, *Advances in Water Resources*, *30*, 576-588, (2007).

Fucik, R., M. J., B. M., and I. T. H., Semianalytical solution for two-phase flow in porous media with a discontinuity, *Vadose Zone*, *7*, 1001-1007, (2008).

Glimm, J., J. W. Grove, X. L. Li, and N. Zhao, Simple front tracking *Contemporary Mathematics*, *238*, edited by G.-Q. Chen and E. DiBenedetto, pp133-149, Am. Math. Soc., Providence, R.I. (1999).

Helmig, R., *Multiphase flow and transport processes in the subsurface; a contribution to the modeling of hydrosystems*, Environmental Engineering., Springer, Berlin, ISBN 3-540-62703-0, pp367, (1997).

Helmig, R., C. Braun, and S. Manthey, Upscaling of two-phase flow processes in heterogeneous porous media: Determination of constitutive relationships, *IAHS AISH Publication*, *277*, 28-36, (2002).

Helmig, R., and R. Huber, Comparison of Galerkin-type discretization techniques for two-phase flow in heterogeneous porous media, *Advances in Water Resources*, *21*, 697-711, (1998).

Hoteit, H., and A. Firoozabadi, Numerical modeling of two-phase flow in heterogeneous permeable media with different capillarity pressures, *Advances in Water Resources*, *31*, 56-73, (2008).

Huang, H., and P. Meakin, Three dimensional simulation of liquid drop dynamics within unsaturated vertical Hel-Shaw cells, *Water Resources Research*, *44*, 10pp, (2008).

Huang, H., P. Meakin, and L. Moubin, Computer simulation of two phase-immiscible fluid motion in unsaturated complex fractures using a volume of fluid method., *Water Resources Research*, *41*, 12pp, (2005).

Ippisch, O., H. J. Vogel, and P. Bastian, Validity limits for the van Genuchten-Mualem model and implications for parameter estimation and numerical simulation, *Advances in Water Resources*, *29*, 1780-1789, (2006).

Istok, J., *Groundwater Modeling by the Finite Element Method*, American Geophysical Union, 2000 Florida Avenue, NW, Washington, DC 20009, (1989).

Juanes, R., and Patzek, T.P., Multiscale-stabilized finite element methods for miscible and immiscible flow in porous media, *Journal of Hydraulic Research*, Vol 42, Extra Issue, 131-140, (2004).

Klieber, W., and B. Riviere, Adaptive simulations of two phase flow by discontinous Galerkin methods, *Computer Methods in Applied Mechanics and Engineering*, *196*, 404-419, (2006).

Kolditz, O. Modelling of flow and heat transfer in fractured rock: Conceptual model of a 3-D deterministic fracture network. Geothermics, 24 (3): 451-470, (1995).

Kolditz, O., Non-linear flow in fractured rock, *International Journal of Numerical Methods for Heat & Fluid Flow*, *11*, 547-575, (2001).

Lewis, R. W., and B. A. Schrefler, *The Finite Element Method in the Static and Dynamic Deformation and Consolidation of Porous Media*, 2 ed., 492 pp., John Wiley & Sons, Chichester, England, (1998).

McDermott, C. I., M. Lodemann, I. Ghergut, H. Tenzer, M. Sauter, and O. Kolditz, Investigation of coupled hydraulic-geomechanical processes at the KTB site: pressure-dependent characteristics of a long-term pump test and elastic interpretation using a geomechanical facies model, *Geofluids*, *6*, 67-81, (2006).

McDermott, C. I., S. A. Tarafder, and C. Schüth, Vacuum assisted removal of volatile to semi volatile organic contaminants from water using hollow fiber membrane contactors II: A hybrid numerical-analytical modeling approach., *J. Membrane Science*, *292*, 17-28, (2007).

McDermott, C. I., R. Walsh, R. Mettier, G. Kosakowski, and O. Kolditz, Hybrid analytical and finite element numerical modeling of mass and heat transport in fractured rocks with matrix diffusion, , *Computational Geosciences, DOI: 10.1007/s10596-008-9123-9*, (2009).

McWhorter, D.B., and D. K. Sunada. Exact integral solutions for two-phase flow. *Water Resources Research*, 26:399–413, (1990).

Meakin, P., and A. M. Tartakovsky, Modeling and simulation of pore-scale multiphase fluid flow and reactive transport in fractured and porous media., *Rev. Geophys.*, *47*, 47pp, (2009).

Niessner, J., and S. M. Hassanizadeh, A model for two-phase flow in porous media including fluid-fluid interfacial area, *Water Resources Research*, 44, W08439, (2008) doi:10.1029/2007WR006721.

Thorenz, C., Model adaptive simulation of multiphase and density driven flow in fractured and porous media. PhD thesis, Universitaet Hannover, 2001, ISSN 0177-9028, pp179, (2001).

Thorenz C, Kosakowski G, Kolditz O and Berkowitz B, An experimental and numerical investigation of saltwater movement in partially saturated systems. *Water Resources Research*, vol. 38(6), (2002), 10.1029/2001WR000364.

Unverdi, S. O., and G. Tryggvason, A Front-Tracking Method for Viscous, Incompressible, Multi-Fluid Flows, *J. Computational Physics.*, *100*, 25-37, (1992).

van Duijn, C.J., and M. J. de Neef, Similarity solution for capillary redistribution of two phases in a porous medium with a single discontinuity. *Advances in Water Resources.*, 21:451–461, (1998).

van Genuchten, M. T., A closed form equation for predicting the hydraulic conductivity of unsaturated soils., *Soil Science Society of America Journal*, *44*, 892-898, (1980).

Versteeg, H. K., and W. Malalasekera, *An Introduction to Computational Fluid Dynamics, The Finite Volume Method*, Second Edition ed., 503 pp., Pearson Prentice Hall, (2007).

Wang, W., and O. Kolditz, Object-oriented finite element analysis of thermo-hydro-mechanical (THM) problems in porous media, *International Journal of Numerical Methods in Engineering*, vol. 69 (1): 162-201, (2007).

Wang WQ, Kosakowski G and Kolditz O, A parallel finite element scheme for thermo-hydro-mechanical (THM) coupled problems in porous media. Computers & Geosciences, vol 35(8): 1631-1641, (2009).

Younes, A., Ackerer, P. and Delay, F. Mixed finite elements for solving 2-D diffusion type equations, Reviews of Geophysics, 48, RG1004/2010 pp 26, (2010).

Zienkiewicz, O. C., and R. L. Taylor, *The Finite Element Method*, 6 ed., 752 pp., Butterworth Heinemann, (2005).

Figure Captions

Table I Fluid properties, models 1,2 & 3

Parameter	Brine	Supercritical CO_2
Density	$1050 Kg/m^3$	$740 Kg/m^3$
Viscosity	0.65×10^{-3}	0.0598×10^{-3}

Table II Material parameters, model 1&3

Parameter	Model 1&2	Model 3
Permeability	$1\times10^{-14} m^2$	$1\times10^{-14} m^2$, $1\times10^{-16} m^2$
Porosity	0.20	0.20

Table III Material parameters model 4 & 5.

Permeability	Model 4	Model 5
$1\times10^{-12} m^2$	12%	8%
$1\times10^{-13} m^2$	18%	17%
$5\times10^{-14} m^2$	18%	16%
$1\times10^{-14} m^2$	20%	16%
$5\times10^{-15} m^2$	11%	17%
$1\times10^{-15} m^2$	21%	17%
$1\times10^{-16} m^2$	-	8%
Porosity	0.2	0.2

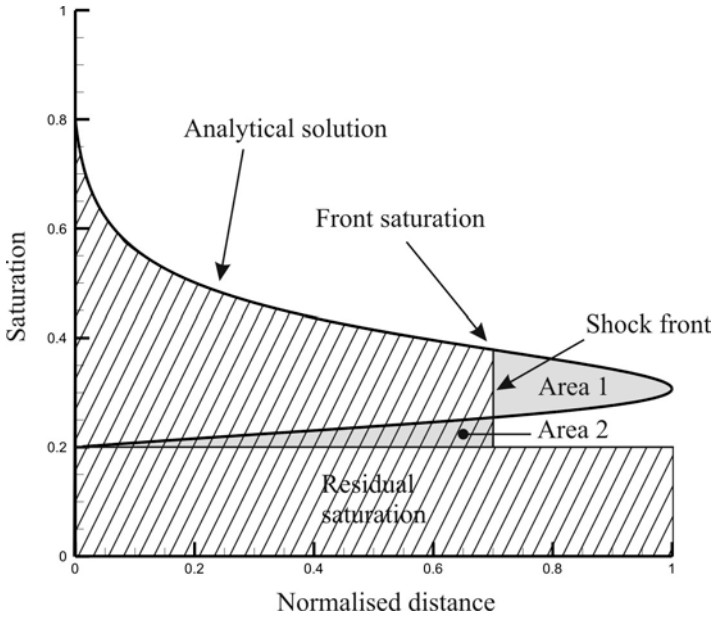

Figure 1 Analytical solution for two phase flow.

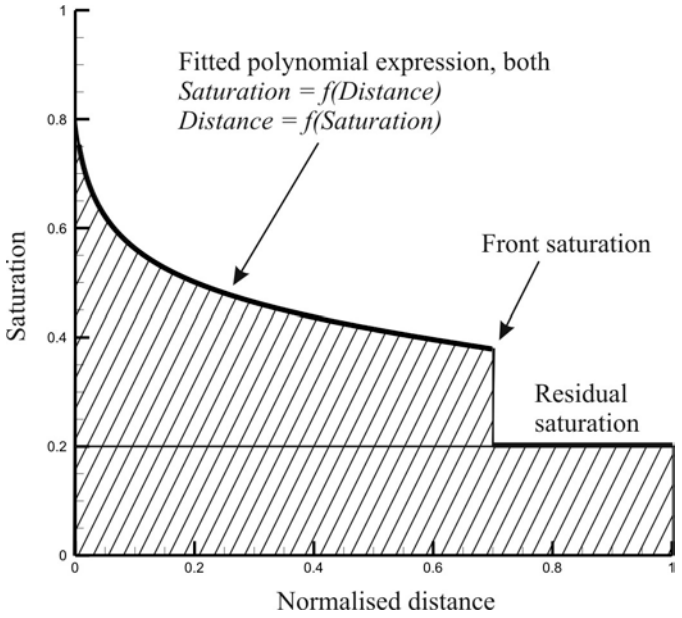

Figure 2 Two phase flow surface is approximated by a polynomial expression.

```
$TPF_ANALYTICAL_CURVEDSURFACE
;Front saturation, Residual saturation, Maximum saturation , Scaling factor,   Polynomial coef. 7 values x^6 x^5 x^4 x^3 x^2 x c
     0.378                0.2                  0.8                  5.1          -275.33  971.28  1375  976.29  -346.05  47.182 0.974
$TPF_ANALYTICAL_INVERSE
; Polynomial coefficients 7 values x^6 x^5 x^4 x^3 x^2 x c
516.45  -973.06  714.0  -258.89  49.222  -5.1998  0.7835
```

Figure 3 Extra input code to trigger and describe the HAN method in OpenGeoSys .

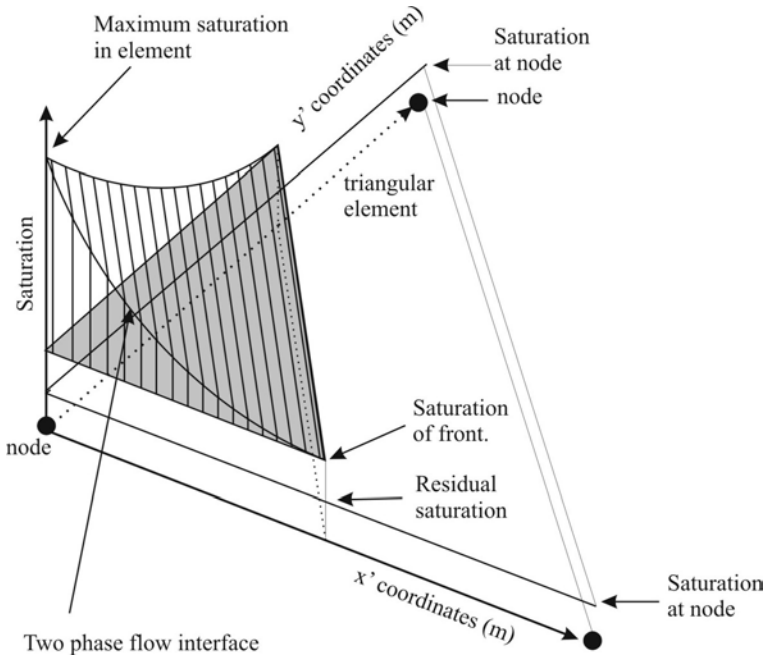

Figure 4 The front has passed one node in the element.

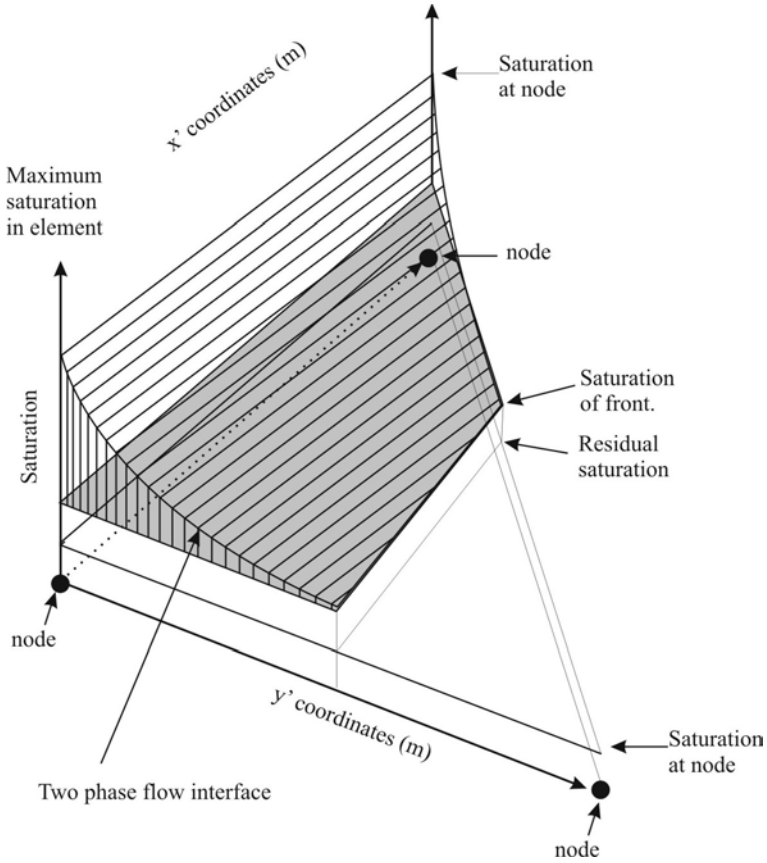

Figure 5 The front has passed two nodes in an element.

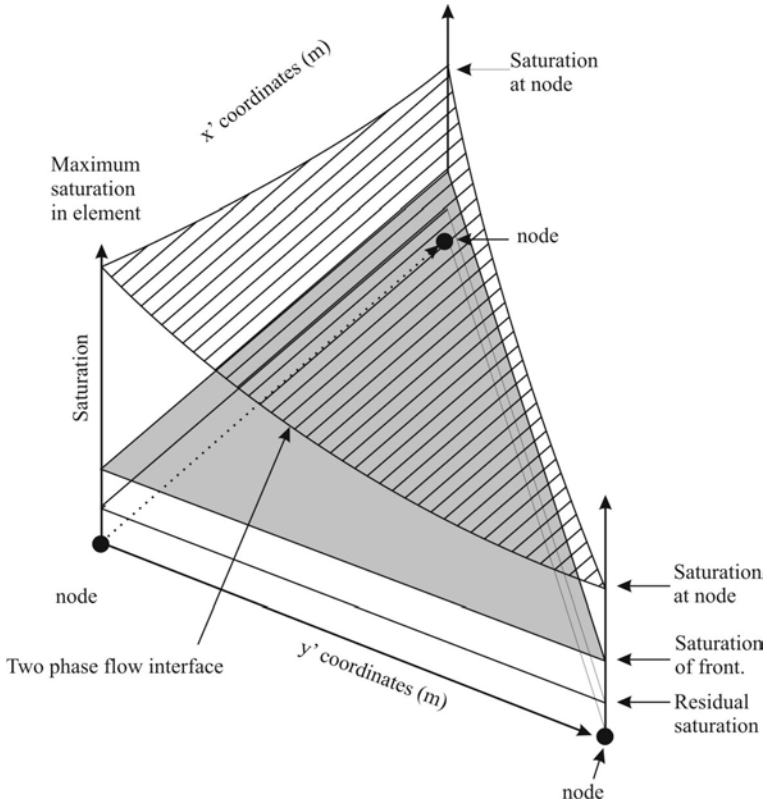

Figure 6 Two phase flow front has passed an element

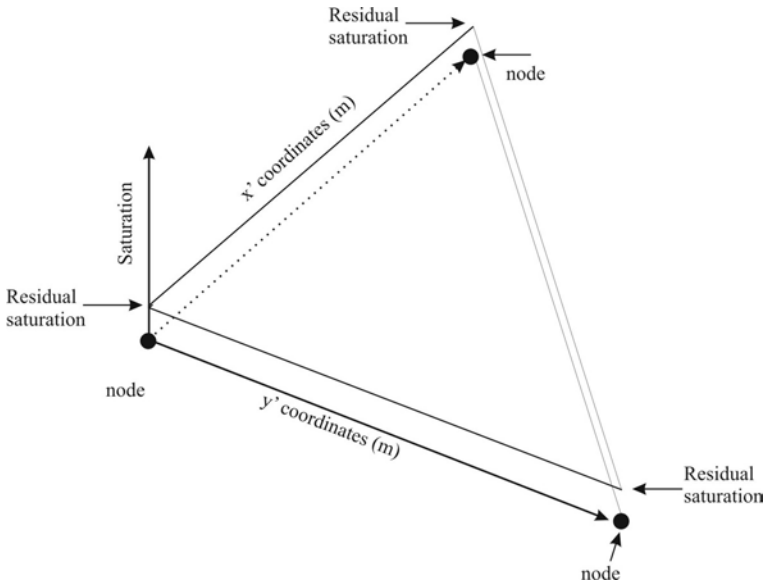

Figure 7 Two phase flow front has not yet reached the element

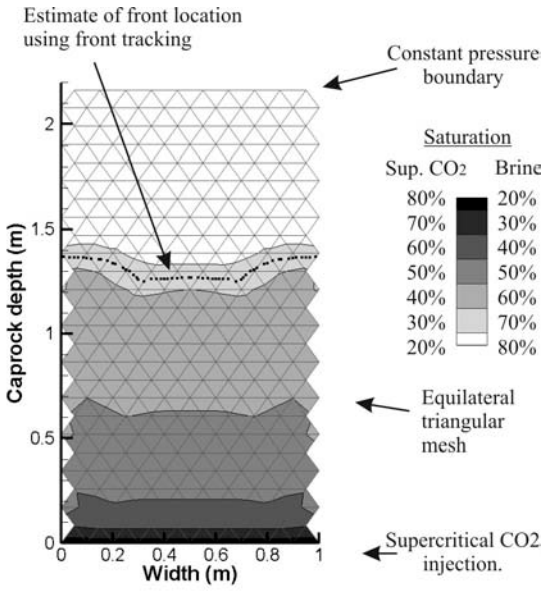

Figure 8 Model for injection of supercritical CO_2 at the base of homogeneous caprock, application of front tracking method.

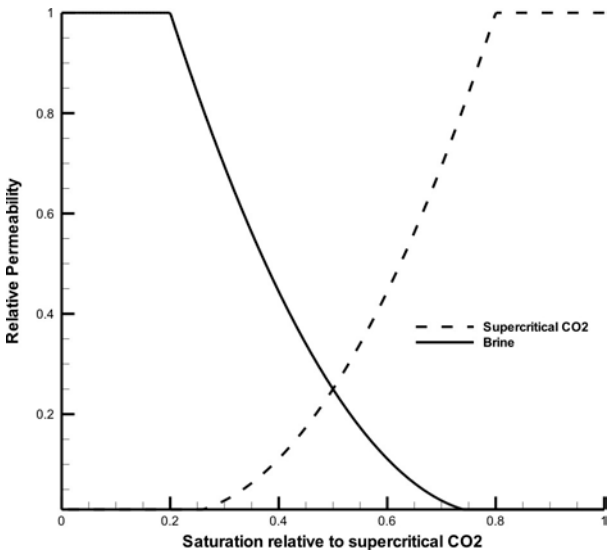

Figure 9 Relative permeabilities functions from *Buckley and Leverett* [1941]

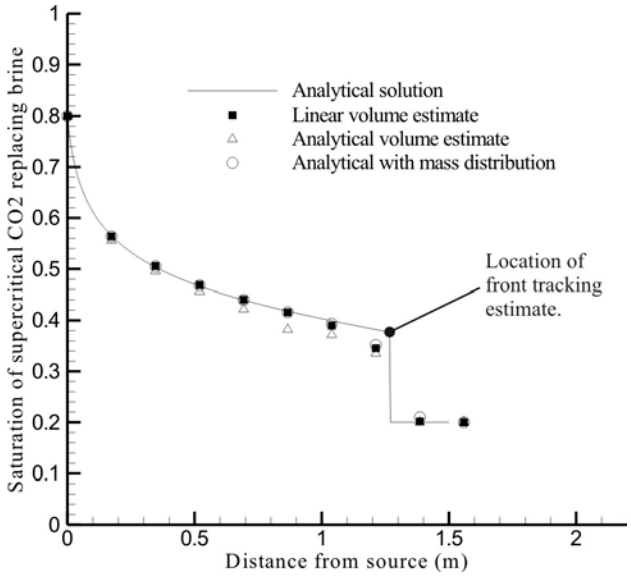

Figure 10 Comparison of the analytical solution to volumetric method, the analytical method with and without mass distribution and the estimation of the front tracking method.

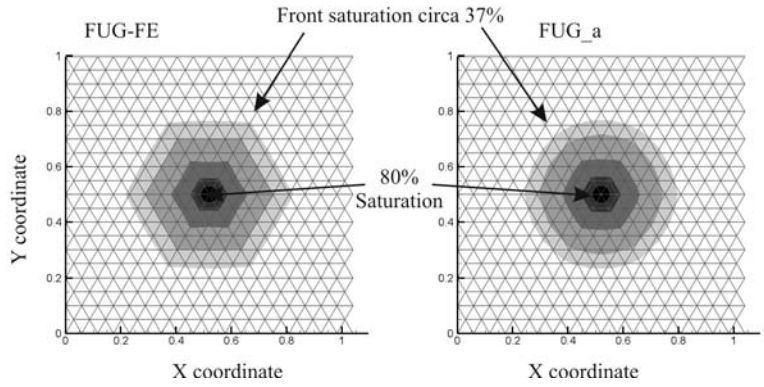

Figure 11 Comparison of radial solutions using the FUG-FE and the FUG-a approaches.

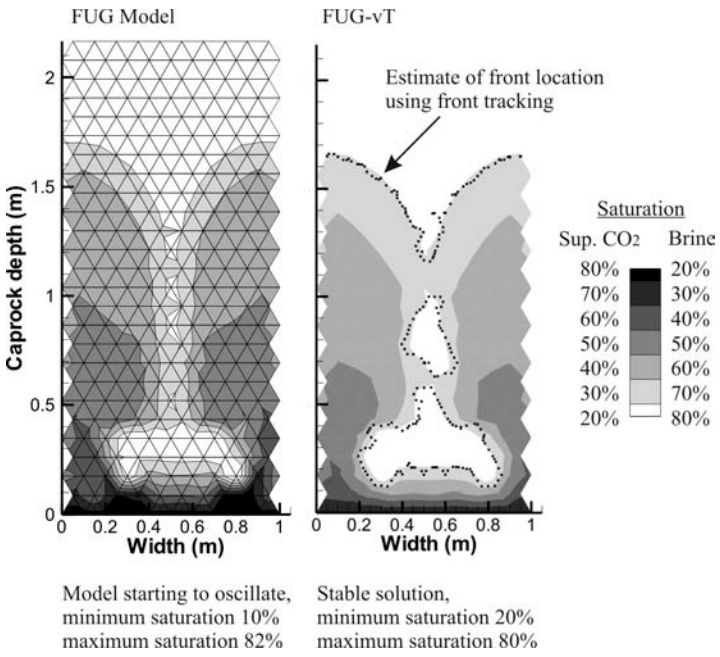

Figure 12 Low permeability layer just above the injection front, comparison of FUG and FUG-vT model performance, 40.5 days after start of forced injection.

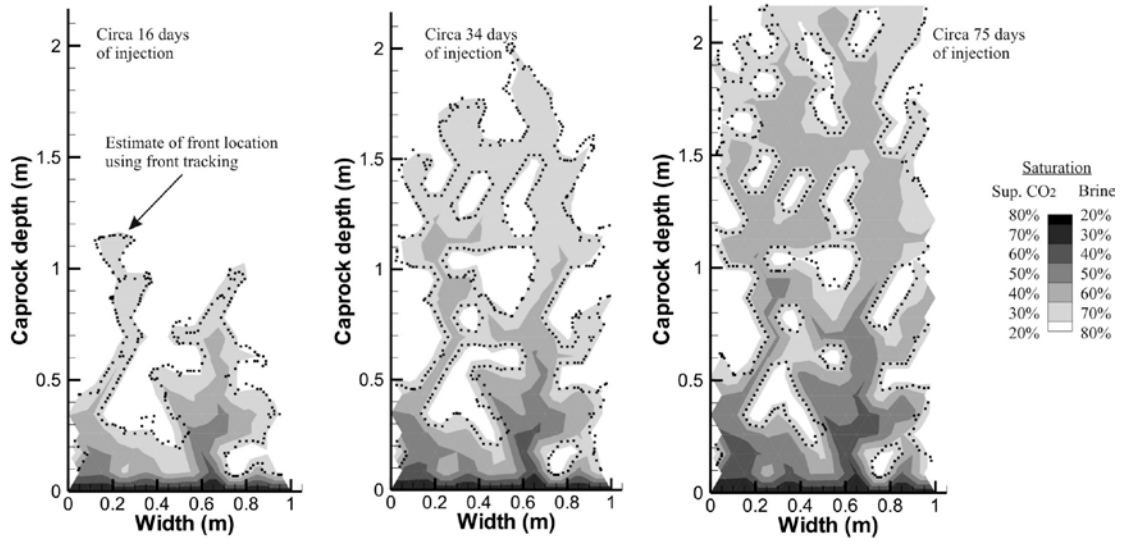

Figure 13 Injection into a heterogeneous field

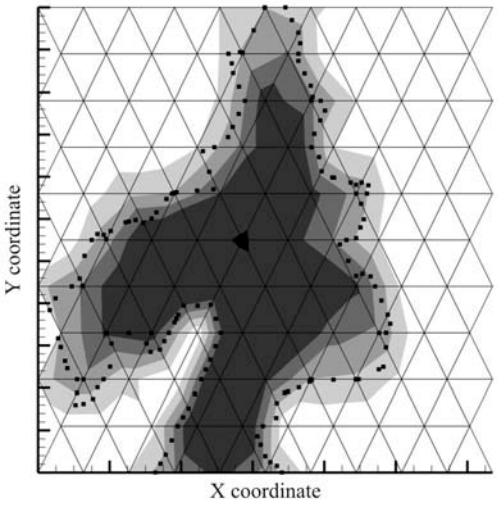

Figure 14 Front tracking provides sub element scale information on the location of the saturation front in a heterogeneous field.

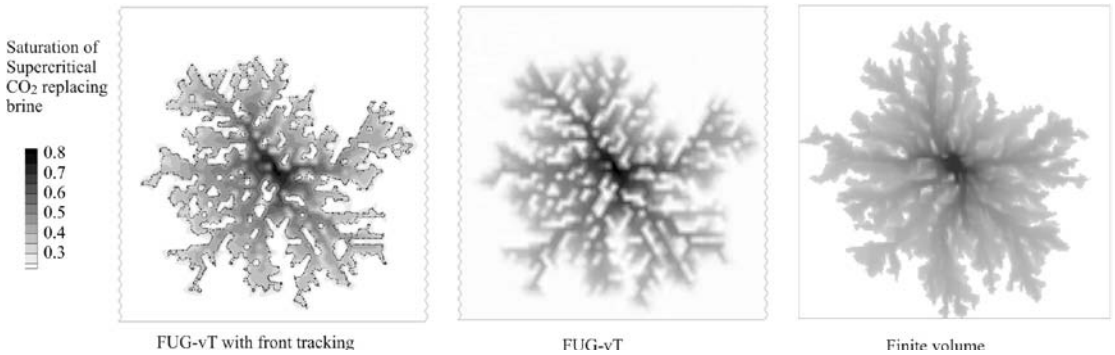

Figure 15 Comparison of well injection of supercritical CO_2 in a heterogeneous reservoir rock with front tracking, then without front tracking and continuous colouring for FUG-vT and a Finite volume solution.